Crisis induced by an escape from a fat strange set

Yue He,[1] Yu-Mei Jiang,[1] Ying Shen,[1] and Da-Ren He[2,1,*]
[1]*College of Physics Science and Technology, Yangzhou University, Yangzhou, China 225002*
[2]*CCAST (World Laboratory), P.O. Box 8730, Beijing, China 100080*
(Received 26 December 2003; revised manuscript received 12 August 2004; published 19 November 2004)

This article reports a characteristic crisis observed in a two-dimensional discontinuous and noninvertible map. The discontinuity border in the definition range of the mapping oscillates as the discrete time progresses so that the forward images of the border form a fat fractal. By choosing particular parameters the iterations on the fat fractal display chaotic motion, and the transient iterations from the initial values in a certain region of the phase space are attracted to the fat fractal. At a threshold of a control parameter an elliptic periodic orbit and the elliptic islands around it suddenly appear inside the fat strange set so that the iterations on the set escape to the islands. The fat chaotic attractor thus suddenly transfers to a fat transient set. The effect of the feature of the crisis on the rule of the lifetime in the transient set is discussed. It shows that the dependence of the lifetime on the control parameter follows a universal scaling law suggested by Grebogy, Ott, and Yorke [Phys. Rev. Lett. **57**, 1284 (1986)], and the scaling exponent can be approximated according to the variation rules of the elliptic islands and the measure of the fat fractal. The strange repeller, which appears after the crisis, is also a fat fractal.

DOI: 10.1103/PhysRevE.70.056213 PACS number(s): 05.45.−a

I. INTRODUCTION

Crisis, which is a common manifestation, means sudden changes of chaotic attractors. Usually the mechanism of the sudden change is the sudden appearance of a so-called escaping hole inside a chaotic attractor when a control parameter reaches a threshold value. As the control parameter progresses, the hole gradually grows, from zero measure, so that the motion in the attractor escapes faster [1–3]. In one of the typical circumstances, in an everywhere smooth dissipative system, the chaotic attractor is the closure of the unstable manifold of a saddle node located in its basin boundary. For a two-dimensional mapping system, the closure forms a thin fractal with a Hausdorff dimension between 1 and 2. At the same time, the closure of the stable manifold of the same saddle (in a homoclinic case) or another saddle (in a heteroclinic case) forms the basin boundary of the chaotic attractor. When the control parameter passes a threshold, the unstable manifold crosses the stable one. Consequently the small region surrounded by the crossing manifolds forms the escaping hole. Based on this understanding Grebogy, Ott, and Yorke deduced the universal scaling law [2] as

$$\langle \tau \rangle \propto |A - A_c|^{-\nu}, \tag{1}$$

where $\langle \tau \rangle$ denotes the averaged lifetime of the iterations in the original chaotic attractor, A is the control parameter of the system, and A_c the threshold of the control parameter. Grebogy, Ott, and Yorke proved that, in an everywhere smooth and "exactly dissipative" mapping system, the scaling exponent should take a value of $\nu=1/2$ in a one-dimensional case, and $1/2 \leqslant \nu \leqslant 3/2$ in a two-dimensional case, depending on the properties of the saddles [2]. There are only a few observed crises that do not obey the scaling law (1). References [3] and [4] may serve as two examples.

In recent years, piecewise continuous maps have attracted much attention. Some different kinds of crises have been observed in such systems [4–6]. Most of these crises obey the scaling law (1) with scaling exponents ν between $1/2$ and $3/2$. However, the values do not depend on the properties of any saddle. The characteristics of the crises still depend on escaping holes, but the mechanisms and forms of the holes are very different. For example, the escaping hole in a so-called hole-induced crisis [4,5] is a hole formed by a pair of discontinuities, which suddenly appear at an extremum of the system function. The escaping hole of the so-called discontinuity-induced crisis can serve as another example [6]. The hole is actually the distance between a discontinuity of the system function, which confines the chaotic attractor, and an unstable orbit located at the basin boundary of the chaotic attractor. Some scientists also paid attention to piecewise continuous conservative systems [7–12]. Among them, Hu *et al.* and Chen *et al.* discussed a system exemplified by a particle in an infinite potential well subject to a periodic kicking force [7,8]. We suggest calling special attention to the crisis observed recently in so-called quasidissipative systems [9–12]. Such a system is described by a discontinuous and noninvertible concatenation of two area-preserving maps. The smooth borderline between the definition ranges of the two submaps is addressed as the "discontinuity border." In certain conditions two points in phase space may merge into one during an iterating process according to different submaps, which induces a collapse of the phase space. However, the phase space contraction rate is linear instead of exponential, as occurs in conventional dissipative systems [12]. In correspondence, the nonasymptotic phase space collapse in quasidissipative systems often is finite. The iterations started from some initial points often enter into elliptic islands, which have finite measures, after a finite time period.

*Author to whom correspondence should be addressed. Address: College of Physics Science and Technology, Yangzhou University, Yangzhou, China 225002.

 ©2004 The American Physical Society

An infinitely long iteration trajectory often is dissipative only at the beginning before a time threshold, and becomes conservative after it. This fact shows that the kind of dissipative behavior can also produce regular attractors, which usually take the form of elliptic islands. A crisis happens when some elliptic islands, which attract iterations, suddenly appear inside a chaotic attractor [11,12].

Mira has analytically proved [13] that in certain kinds of two-dimensional piecewise continuous noninvertible maps, like the system to be discussed in this article, the chaotic area is bounded by segments of images of the discontinuity borderlines. If the border is a smooth line in the definition range, the set of the images of the borderline forms a thin fractal with a Hausdorff dimension between 1 and 2 when the number of images tends to infinite. As a result the chaotic motion is confined in the fractal in this case. After a crisis occurring in a quasidissipative mapping, the chaotic attractor appears, which is formed by the borderline image set.

After all of the aforementioned crises, the backward image set of the escaping hole cuts out nearly all the points of the original chaotic attractor. The remnants form a fractal set with a Hausdorff dimension smaller than that of the original attractor. The set is addressed as a chaotic saddle [1,14] or a strange repeller [15]. Trajectories starting from points of a strange repeller never leave the repeller and exhibit chaotic motion forever. It is, however, completely unlikely to hit such a point by random choice since the repeller is a set of zero measure and is globally not attractive. What is observable experimentally is not the repeller itself but rather a small neighborhood of it. Trajectories starting close to the repeller can stay for a long time in its neighborhood and show chaotic properties, but sooner or later they escape. Therefore a chaotic saddle or strange repeller leads to transient chaos. The averaged lifetime of the chaotic transient can be arbitrarily long in some circumstances. In a low dimensional chaotic system so-called supertransients, meaning that the averaged lifetime is arbitrarily large, usually only occur in an arbitrarily small parameter interval in the vicinity above the crisis threshold [1,16]. In contrast, Crutchfield and Kaneko discovered that in spatiotemporal chaotic systems supertransients occur commonly in substantial portions of the parameter space [17,18]. Lai and Winslow demonstrate that this fact is due to nonattracting chaotic saddles whose stable manifold measures have fractal dimensions that are arbitrarily close to the phase space dimension [16]. We may say that the chaotic saddle's stable manifolds are arbitrarily close to fat fractals. Properties of chaotic saddles or strange repellers and chaotic transients are important physical quantities in practical fields, such as controlling chaos [19] and sustaining chaos [20].

In this article we suggest a different mechanism that may also produce supertransients. For this we shall report a sample crisis, which leads to supertransients by the mechanism, and then argue that the mechanism may be widely observed. The paper is organized as follows. The system is described in Sec. II. The crisis is discussed in Sec. III where a fat chaotic attractor and its sudden vanishing are discussed in Sec. III A, our analytic discussion about the lifetime scaling law is introduced in Sec. III B, and the numerical verification is introduced in Sec. III C, and the strange repeller and its variation as the control parameter changes are described in Sec. III D. A summary and discussion are presented in the last section.

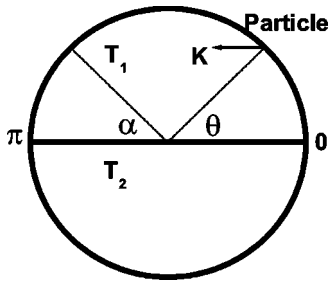

FIG. 1. A schematic drawing to show the system.

II. THE SYSTEM

The kicked rotor is a widely used theoretical model that displays important features such as onset of chaos, phase locking, and so on. Schuster showed that the differential equations which describe the motion of the system can be reduced to a two-dimensional map. Taking different limits, the map can change to some famous models, such as the logistic map, the Hénon map, and the standard map (Chirikov-Taylor map) [21]. The last one, the standard map, may be the simplest paradigm to show the basic characteristics of chaotic motion in a conservative system. In 1979, Chirikov derived the standard map by considering the motion of a charged particle in a magnetic bottle [22]. In 1997 Blumel and Reinhardt suggested a much simpler experimental setup for realization of a kicked rotor. They considered a two-dimensional dipole, which is driven by an electric field generated by a special zero-width pulse generator, and again derived the standard map [23]. The standard map can be derived through very different physical models. For example, Wang *et al.* derived it by considering an electronic relaxation oscillator [9]. In the following we shall discuss a two-dimensional map that is a discontinuous and noninvertible concatenation of two standard maps in different forms. A special kind of kicked rotor is considered only as one of the possible backgrounds of the map. Similar maps with similar important features may be derived in other ways.

Similar to the systems discussed in [7,8,12], we consider a kicked rotor, in which a classical particle moving without friction along a unit circle is subjected to a periodic impulsive force of impulse strength K. As shown in Fig. 1, the direction of the force is parallel to the diameter that connects two positions $\theta=0$ and $\theta=\pi$, where θ denotes the angular position of the particle. The periods of the impulses, T_i $(i=1,2)$, are different in the definition range $\theta\in(0,\alpha]$ (for T_1) and $\theta\in(\alpha,2\pi]$ (for T_2). Along the tangent direction of the circle, the impulsive forces can be expressed as

$$F_{1\tau}=(K\sin\theta)\delta_{T_1}(t)\ \ (0<\theta\leqslant\alpha),$$

$$F_{2\tau}=(K\sin\theta)\delta_{T_2}(t)\ \ (\alpha<\theta\leqslant 2\pi), \tag{2}$$

where $\delta_{T_i}=\Sigma_{n=-\infty}^{\infty}\delta(t-nT_i)$. With some kinds of technologies (for example, in the driven two-dimensional dipole model

suggested by Blumel and Reinhardt [23] the frequency of the zero-width pulse generator can be controlled by a modern electronic device), the particle can be tracked so that after subjection to an F_i impulse, the next impulse applies only after T_i time duration whether or not it crosses the discontinuity border. This means that the system has a type of "memory" so that the particle may make a free motion in a time duration longer than T_2 in $\theta \in (\alpha, 2\pi]$ if $T_2 < T_1$, and vice versa. For example, if $T_2 = T_1/2$, after last kicking at a position near to the border $\theta = \alpha$ in the upper semicircle, the particle will make a free motion in a T_1 time duration even if it moves, after crossing the border, in $\theta \in (\alpha, 2\pi]$ longer then $T_1/2$.

By integrating the impulse along the tangent direction of the circle and the angular momentum of the moving particle from just before the nth kick to just before the $(n+1)$th kick, one gets

$$\left.\begin{aligned} \theta_{n+1} &= \theta_n + I_{n+1} \pmod{2\pi} \\ I_{n+1} &= I_n + k \sin\theta_n \end{aligned}\right\} \text{ if } 0 < \theta_n \leqslant \alpha, \quad (3)$$

$$\left.\begin{aligned} \theta_{n+1} &= \theta_n + \beta I_{n+1} \pmod{2\pi} \\ I_{n+1} &= I_n + k \sin\theta_n \end{aligned}\right\} \text{ if } \alpha < \theta_n \leqslant 2\pi, \quad (4)$$

where $I = pT_1/m$, $k = KT_1/m$, $\beta = T_2/T_1$, p denotes the momentum along the tangent direction of the circle, and m denotes the mass of the particle. In the current study we define $\alpha = \pi + A\cos(\omega n)$; this means that the discontinuity border oscillates as the discrete time advances. When $\beta = 1$, maps (3) and (4) are piecewise continuous, conservative, and invertible. When $\beta \neq 1$, the maps become noninvertible and quasidissipative as explained in the first section.

One can easily verify that both the submaps (3) and (4) are area preserving. Also their inverse maps can be deduced easily as

$$\left.\begin{aligned} \theta_n &= \theta_{n+1} - I_{n+1} \pmod{2\pi} \\ I_n &= I_{n+1} - k \sin\theta_n \end{aligned}\right\} \text{ if } 0 < \theta_n \leqslant \alpha, \quad (5)$$

$$\left.\begin{aligned} \theta_n &= \theta_{n+1} - \beta I_{n+1} \pmod{2\pi} \\ I_n &= I_{n+1} - k \sin\theta_n \end{aligned}\right\} \text{ if } \alpha < \theta_n \leqslant 2\pi. \quad (6)$$

Please note that in order to find an inverse image (θ_n, I_n), the principal for selecting Eq. (5) or Eq. (6) depends on the position θ_n instead of θ_{n+1}. This leads to the possibility of finding two (θ_n, I_n) points for the same (θ_{n+1}, I_{n+1}) according to the different inverse mapping form. This is the so-called noninvertibility induced by discontinuity, which is the source of the quasidissipative property.

There are two discontinuity borderlines $\{(\theta, I)|_{\theta=0}\}$ and $\{(\theta, I)|_{\theta=\alpha}\}$ in maps (3) and (4). The second one is a linear line that can take values continuously in the area $\{(\theta, I)|_{\theta \in [\pi - A, \pi + A]}\}$ so that the border image set forms a fat fractal.

The fixed-point solutions of maps (3) and (4) are

$$\left.\begin{aligned} I^* &= 0 \\ \theta^* &= \pi \end{aligned}\right\} \text{ when } 0 < \theta_n \leqslant \alpha, \quad (7)$$

$$\left.\begin{aligned} I^* &= 0 \\ \theta^* &= 2\pi \end{aligned}\right\} \text{ when } \alpha < \theta_n \leqslant 2\pi. \quad (8)$$

In the definition range $(0, \alpha]$ it exists and is stable when $A = 0$ and $|(2 - k \pm \sqrt{k^2 - 4k})/2| \leqslant 1$ while in $(\alpha, 2\pi]$ it exists and is stable when $|[2 + \beta k \pm \sqrt{\beta k(\beta k + 4)}]/2| \leqslant 1$.

One has to discuss the period-2 orbits of maps (3) and (4) for different situations. If both the periodic points are located in $(0, \alpha]$, the solution satisfies

$$I_1 = (2n+1)\pi,$$

$$\theta_1 = \arcsin\left(\frac{-2(2n+1)\pi}{k}\right), \quad (9)$$

$$I_2 = I_1 + k \sin\theta_1,$$

$$\theta_2 = \theta_1 + I_2, \quad (10)$$

where n takes values 0, 1, 2,…. If both the periodic points are located in $(\alpha, 2\pi]$, the solution satisfies

$$I_1 = \frac{(2n+1)\pi}{\beta},$$

$$\theta_1 = \arcsin\left(\frac{-2(2n+1)\pi}{\beta k}\right), \quad (11)$$

$$I_2 = I_1 + k \sin\theta_1,$$

$$\theta_2 = \theta_1 + \beta I_2, \quad (12)$$

where n takes values 0, 1, 2,…. If one periodic point is located in $(0, \alpha]$, and another is located at $(\alpha, 2\pi]$ (the orbit can be addressed as an "orbit crossing border"), the solution satisfies

$$(\beta + 1)(I_1 + k \sin\theta_1) + \beta k \sin(\theta_1 + I_1 + k \sin\theta_1) = 2\pi,$$

$$\theta_1 = n\pi + \frac{\beta I_1}{2}, \quad (13)$$

$$I_2 = I_1 + k \sin\theta_1,$$

$$\theta_2 = \theta_1 + \beta I_2, \quad (14)$$

where n takes values 0, 1, 2,… .

In this article, we only discuss the situation where the parameters are fixed as $k = 0.3$, $\beta = 0.1$, and $\omega = 1$. The control parameter is the amplitude of the oscillation of the discontinuity border, A. It is easy to deduce that the fixed point described by Eq. (7) exists only if $A = 0$, but it is unstable; the fixed point described by Eq. (8) always exists, and also is unstable; both of the periodic orbits described by Eqs. (9), (10), (11), and (12) do not exist; the only existing and stable periodic orbit is that described by Eqs. (13) and (14). There are many such periodic orbits, described by different n, in the phase space. We shall study only the case $n = 1$. The expression of the orbit can be solved as

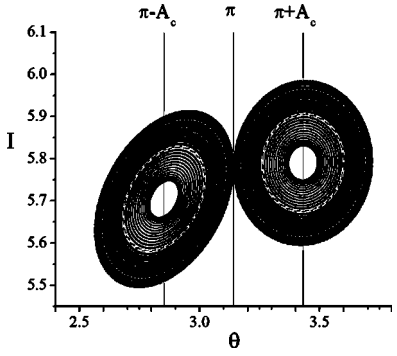

FIG. 2. The elliptic islands around the period-2 orbit. The vertical linear line denoted by π represents the discontinuity borderline $\{(\theta,I)|_{\theta=\alpha}\}$ at $A=0$. The line denoted by $\pi-A_c$ represents one of the two end positions of the borderline at $A=A_c$, when it collides with one of the elliptic points.

$$\theta_1 \simeq 2.852\,10, \tag{15}$$

$$I_1 \simeq 5.704\,20,$$

$$\theta_2 \simeq 3.431\,08, \tag{16}$$

$$I_2 \simeq 5.789\,84.$$

Figure 2 shows the "elliptic islands" around the periodic points. It is drawn by evenly selecting 40×55 initial values in the area $\theta\in[0,2\pi]$, $I\in[5.3,6.1]$ (inside the basin of this orbit), ignoring the first 30 iterations from each initial point, and then recording 100 iterations. The picture shows that the "elliptic island chain" is the attractor in part of phase space due to the fact that it attracts the iterations from all the initial points. In the following sections we shall select different suitable areas for initial values for similar reasons and shall not explain them again.

III. THE CRISIS

A. The fat strange set

As can be understood by Fig. 2, the elliptic islands become smaller and smaller with increasing A. All the elliptic orbits colliding with the oscillating border are destroyed. Finally, the border collides with one of the periodic points at $A=A_c$ (it can be analytically shown that $0.289\,49>A_c>0.289\,48$). As a result, the regular motion totally disappears. Numerical investigation (see Fig. 3) shows that a chaotic attractor suddenly emerges. This sudden change can be addressed as a kind of crisis.

As stated in the first section, the set of forward images of the discontinuity border forms the chaotic attractor. Figure 4 shows the first, second, 20th, 100th, and 1000th to 6000th orders of images of the discontinuity borderline $\{(\theta,I)|_{\theta=\alpha}\}$. One can see that the border image splits and bends again and again during the iteration process, and gradually demonstrates the form of a fat strange set. If the border were one (or two) fixed linear line(s), the image set would have been a thin fractal. However, in the current system one of the borderlines $\{(\theta,I)|_{\theta=\alpha}\}$ changes its position in the region $\theta\in[\pi-A,\pi+A]$ continuously. Since the period (2π) of the function $\alpha=\pi+A\cos(\omega n)$ is an irrational number, the border should perform an ergodic motion in this rectangular area. This is why one can expect that the image set forms a fat fractal. This conclusion should be verified by some numerical proofs, which will be presented in the following.

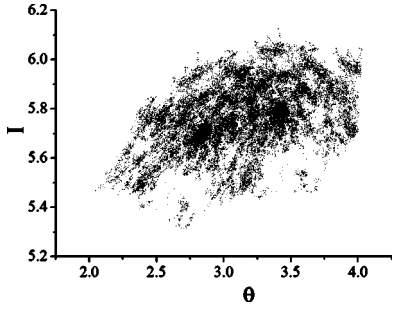

FIG. 3. The chaotic attractor at $A=0.289\,49$. It is drawn by selecting evenly 5×5 initial values in the area $\theta\in(\pi-A,\pi+A)$, $I\in(5.3,6.1)$, ignoring the first 300 000, and then recording 5000 iterations.

First, if the image set is a fat fractal, when one selects m initial values evenly on the border $\{(\theta,I)|_{\theta=\alpha}\}$ and computes l orders of images from each initial value, one certainly finds that the whole image set has a Hausdorff dimension $D_f=2$ (the dimension of the phase space where it is embedded) with a good enough computational resolution and $m\to\infty$, $l\to\infty$. To verify this conclusion numerically, we computed the Hausdorff dimension of the fat strange set shown by Fig. 3 by using the traditional box-counting method. The phase space shown in the figure was divided into 400×400 squares. We took the size of one square as the smallest scale l. The number of points showing the strange set is about 100 times the number of squares. When we increase the scale, the number of boxes occupied by the fractal, N, showed a very good linear line on the $\ln l$-$\ln N$ plane. The slope of the line was $2\pm5\times10^{-16}$. Therefore, the Hausdorff dimension is not a good quantity to describe the border image set here. One has to introduce a different quantity that is suitable for both the thin and fat fractals. It is called the "fractal exponent" and is defined as [24–26]

$$\beta=\lim_{\xi\to0}\frac{\ln|\mu(A_\xi)-\mu_0|}{\ln\xi}, \tag{17}$$

where ξ denotes the scale, A_ξ represents the coarse set of the fat fractal under ξ (this means the remnant after wiping off all the holes larger than ξ), $\mu(A_\xi)$ represents the Lebesque measure of A_ξ, and μ_0 the limit of $\mu(A_\xi)$ when $\xi\to0$, i.e., $\mu_0=\lim_{\xi\to0}\mu(A_\xi)$. Figure 5 shows the computation of the fractal exponent for the fat strange set shown in Fig. 3. One can see a good scaling-free region in the figure. The fractal exponent is then obtained as $\beta=0.414\pm0.006$.

When the fat fractal A_ξ gradually changes to a thin one, one should find $\mu_0|_{\text{thin}}=\lim_{\xi\to0}\mu(A_\xi)|_{\text{thin}}=0$ [25,26]. As is well known [25], in this case one finds $\mu(A_\xi)=\xi^\beta=\xi^{D-D_f}$, where D is the dimension of the space where the fractal is

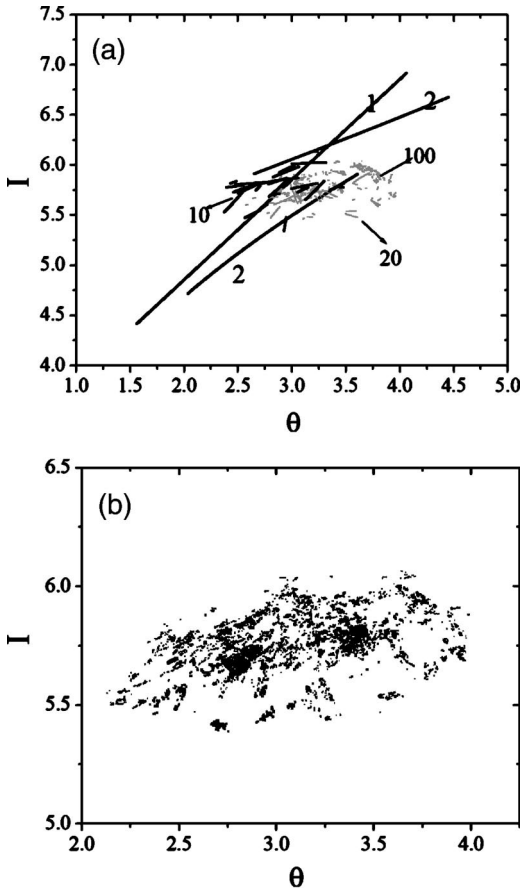

FIG. 4. (a) The linear line 1 represents the first image of the discontinuity border $\{(\theta,I)|_{\theta=\alpha}\}$. It is drawn by selecting evenly 5000 initial values in the region $\theta=\pi+A$, $I\in(4.5,7)$, and recording the first iteration from each of them. Two linear lines, denoted by 2, represent the second images of the border. The drawing method is similar so we shall not explain it in the following. The small gray segments represent the 20th images, and the small gray pieces represent the 100th images. They already roughly resemble the fat strange set shown in Fig. 3. (b) The composition of 1000, 2000, 3000, 4000, 5000, and 6000 order images of the discontinuity border. It already has a very similar form to the strange set shown in Fig. 3, and has a tendency to show a form of composition of small pieces. In order to compare with Fig. 3, all the computations are performed with parameter value at $A=0.289\,49$.

embedded, D_f denotes the Hausdoff dimension of the thin fractal. In the current system, when $A=0$, the border does not oscillate. It can be expressed as $\alpha=\pi$. The fat fractal set changes to a thin one. We should find $\beta+D_f=2$. This is the second and most important proof for the fat strange set. We also numerically verified this conclusion. By using a similar method, we computed the Hausdorff dimension of the fat strange set at $A=0$, which now transfers to a transient set, and obtained $D_f=1.226\pm0.016$. The fractal exponent of the set is found to be $\beta_0=0.77\pm0.02$. So the results show a good agreement with the conclusion $\beta+D_f=2$.

B. An analytical discussion of the lifetime scaling law

We have reported a conclusion elsewhere [12] that in a quasidissipative system, due to the dissipative behavior showing a linear time dependence, the phase space contraction rate does not influence the scaling exponent of crises and thus one can approximate the lifetime scaling law for a crisis based only on the formula

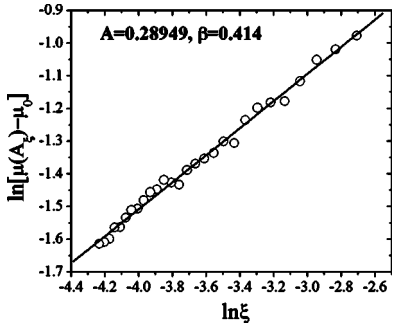

FIG. 5. The computation of the fractal exponent of the fat strange set shown in Fig. 3. The largest value of ξ is 0.0667. Its smallest value is 0.0143, $\mu_0=0.003\,35$. Both μ and ξ have arbitrary square or length units.

$$\langle\tau\rangle\propto\frac{1}{\rho\Delta}, \tag{18}$$

where Δ denotes the measure of the escaping hole, which is the area of the elliptic islands in the current study, and ρ denotes the probability of visiting a unit area in Δ. In the present situation the area of the elliptic islands, which are escaping holes, increases due to the fact that a linear line [the discontinuity borderline $\{(\theta,I)|_{\theta=\alpha}\}$], which should be tangent to the islands all over the process, moves away from them as A becomes smaller. We have numerically verified and confirmed the obvious conclusion

$$\Delta\propto(A_c-A)^2. \tag{19}$$

If the strange set from which iterations escape via a leaking hole is a thin fractal, it has a zero measure. The part of the strange set inside Δ is very uneven no matter how small Δ is. Usually, one has to calculate the dependence of very uneven ρ on $|A-A_c|$ numerically. We shall discuss the reason further below. However, in the current study, the strange set is a fat fractal with a finite measure, we may prove that the part of the strange set inside Δ is even when Δ is small enough and make a further estimation on the scaling exponent based on this fact.

The "density" of a fractal F at a point x can be defined as [27]

$$M=\lim_{\gamma\to0}\frac{\text{area}(F\cap B_\gamma(x))}{\text{area}(B_\gamma(x))}, \tag{20}$$

where $B_\gamma(x)$ is a closed disk with radius γ and a center at x, and area ( ) represents the measure of the set in the parentheses. It has been proven [27] that $M=1$ if $x\in F$, and $M=0$ if $x\notin F$, when F has an integer dimension, while M is smaller than 1 and depends on the Hausdorff dimension of F if it is a thin fractal. The Hausdorff dimension of the thin fractal strange set should vary when the parameter changes. That is why an estimation of ρ is difficult if we suppose that it is proportional to the fractal density M of the strange set.

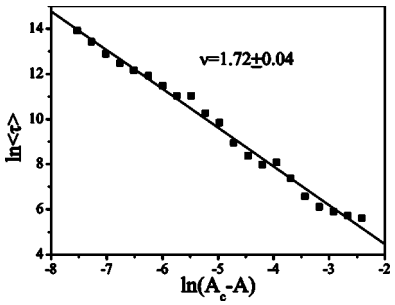

FIG. 6. This figure shows the numerically obtained relationship between the average lifetime $\langle\tau\rangle$ and the controlling parameter.

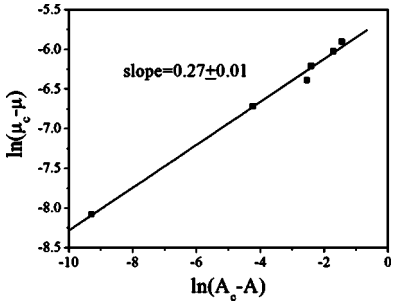

FIG. 7. This figure shows the numerical results about the dependence of $\mu_c-\mu$ on A_c-A. The method is as follows. For each A value, select evenly 100×100 initial values in the area $\theta\in[0,2\pi]$, $I\in[5.3,6.1]$, record all the transient iterations (those before entering the elliptic islands), and then use the data for computing the Hausdorff dimension of the transient set by the box-counting method. Choose the measure value at the smallest scale in the scale-free region as the measure of the transient strange set, μ. Only the measure values corresponding to six parameter values were computed since the computation needs a lot of time. The threshold value of the measure was taken as $\mu_c=0.003\,86$ when $A=A_c=0.289\,492$. It was obtained by considering the fact that the fractal exponent of the set is $\beta=0.414$ at $A=A_c=0.289\,492$. A is dimensionless. μ has arbitrary square units.

However, for the fat strange set F, when $|A-A_c|\to0$, Δ almost always falls in a piece of the set which has a dimension 2, i.e., $\Delta\in F$; therefore $\rho=1$ should be measured. That means the visiting probability should be 100% as soon as iteration enters the fat strange set. With this conclusion and Eqs. (18), (19) one can expect to observe the universal power law expressed by Eq. (1) with an extremely large scaling exponent $\nu=2$. As discussed in Ref. [28], a larger ν makes the chaotic transient phenomena somewhat easier to observe. Therefore one can expect a superlong chaotic transient after the crisis.

C. The numerical verification of the lifetime scaling law

Figure 6 shows our computational results for the averaged lifetime, by using the method

$$\langle\tau\rangle=\lim_{n\to\infty}\frac{\sum_{i=1}^{n}\tau_i}{n}, \tag{21}$$

where n denotes the number of initial values evenly chosen in area $\theta\in[2,4]$, $I\in[5.1,6.3]$ (here $n=100\times100$), and τ_i denotes the number of iterations before entering the elliptic islands from initial value i. The linear line in the figure represents the least squares fitting of the data. Its slope is the exponent of the scaling law, which shows $\nu=1.72\pm0.04$.

Our task now is finding an explanation of the difference between the analytically predicted scaling exponent $\nu=2$ and the numerical result. We would like to make a guess. Although we obtain the conclusion that the probability of the iterations visiting the escaping hole should be 100% as soon as the iteration enters the fat strange set, we may have to consider the probability of the iterations visiting the fat strange set since it does not occupy the whole phase space. When the parameter A progresses, the averaged lifetime $\langle\tau\rangle$ should be longer if μ, the measure of the strange set at parameter value A, decreases since it takes a longer time for iterations to enter the strange set. We suppose that $\langle\tau\rangle$ is proportional to $(\mu_c-\mu)$ (μ_c is the measure at the crisis threshold). This variation influences the scaling exponent only if the dimensionless parameter $\varrho=(\mu_c-\mu)/\mu_c$, the ratio of the measure's change, obeys a power dependence on the parameter A_c-A. Usually it is impossible to make an analytic discussion of this guess because the measure's change sensitively depends on the system function and parameters. We have to verify it numerically.

Figure 7 shows our numerical results about the dependence of $\mu_c-\mu$ on A_c-A. It shows a power law:

$$(\mu_c-\mu)\propto(A_c-A)^{-0.27\pm0.01}. \tag{22}$$

Then we can reach agreement with the numerical result for the scaling exponent if we suggest a different formula for the estimation of the lifetime scaling exponent:

$$\langle\tau\rangle\propto\frac{\varrho}{\rho\Delta}. \tag{23}$$

D. The strange repeller and its fractal exponent

How to show a strange repeller in a figure has been a research subject in nonlinear dynamics. In the current study we use a rather simple method, the "single trajectory method," which was suggested by Tél in 1991 [15]. Figure 8 shows a strange repeller that is drawn with the parameter value at $A=0.20$ in the following way: from a lot of initial values (as many as possible; here the number is 1000

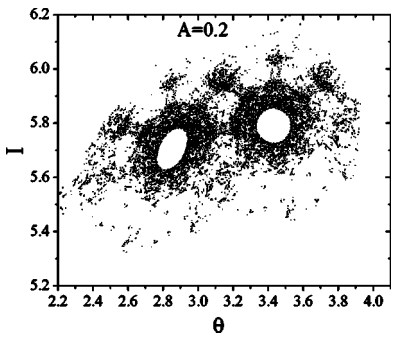

FIG. 8. The strange repeller at $A=0.2$.

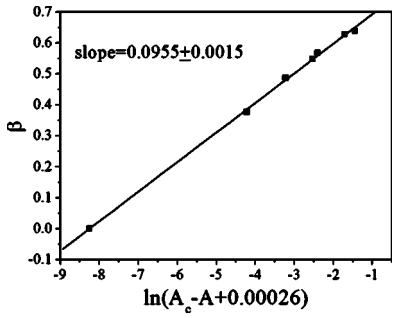

FIG. 9. Variation of the fractal exponent of the strange repeller.

$\times 1000$), selecting those that show lifetimes 15 times longer than the averaged lifetime $\langle\tau\rangle$, and then recording the transience which started from them but ignoring the first 20% to avoid the "memory of the initial condition" and the last 40% to avoid getting too near to the new attractor, the elliptic islands. The recorded middle part of the transient can approximately show the strange repeller as explained in the first section. We compute the fractal exponents β of some strange repellers in the parameter range $A \in [0.055, 0.275]$ and show the data in Fig. 9. In the computation for each of them, the smallest value of ξ is 0.0143, the largest value is 0.0667, and 55 values of ξ in total are evenly taken between them. For different values of A, μ_0 takes different values as well. They are $\mu_{0(A=0.055)}=0.001\,13$; $\mu_{0(A=0.11)}=0.001\,45$; $\mu_{0(A=0.2)}=0.001\,85$; $\mu_{0(A=0.21083)}=0.002\,18$; $\mu_{0(A=0.275)}=0.003\,15$. The results show that the fractal exponents are increasing with decreasing A with the rule

$$\beta = -(0.0955 \pm 0.0015)\ln(A_c - A + 0.000\,26). \quad (24)$$

These results demonstrate that the strange repellers are also fat fractals. This can explain the superlong transience (longer than 6×10^5) observed when $|A-A_c|\to 0$. Obviously the supertransients occur in a portion of the parameter space that is much larger than what can be observed after a crisis induced by an escape from a thin strange set.

IV. CONCLUSION AND DISCUSSION

The system discussed in this article is described by a two-dimensional mapping. Two linear lines in the definition range of the system divide the range into two parts as shown in Fig. 1. The function is different in each part. One of the borderlines is fixed; the other oscillates with a certain amplitude. This mechanism makes the chaotic set of the borderline image become a fat fractal. Due to the quasidissipative property of the system, a zero-size elliptic island chain appears inside the chaotic set at a threshold value of the control parameter. The island chain gradually grows and serves as an escaping hole so that the chaotic set transfers to a transient set. The characteristic of this crisis is an escape from a fat fractal set. We have analytically and numerically shown that the scaling exponent of the lifetime takes a value of 1.73. The method for the estimation of the exponent is unique.

The crisis reported in this paper is only an example to show that a kind of crisis induced by an escape from a fat strange set can be observed, and this can display a different mechanism to produce supertransients. The key point is that the strange repeller, which appears after such a crisis, is also a fat fractal. Therefore the iterations have a much larger probability than that in the thin fractal case to fall in the vicinity of the strange repeller. We believe there should be more mechanisms to realize this kind of crisis, not only in two-dimensional discontinuous and noninvertible maps. Also, the mechanism reported in this paper certainly can be observed in more physical systems, which can show an oscillation of a discontinuous borderline and thus form a fat strange set. The electronic relaxation oscillator reported in Ref. [9] and the so-called kicked billiard model [29] might serve as other candidates. So we believe that the mechanism for producing supertransients is common.

ACKNOWLEDGMENTS

This study was supported by the National Natural Science Foundation of China under Grant No. 10275053. The authors would like to thank Professor Kangjie Shi at Northwest University, China for very helpful discussion and suggestions. Also, the manuscript was completed in the Department of Computational Science, National University of Singapore. D.-R.H. wants to express his gratitude to Professor K. Chen for providing advanced research facilities and valuable financial support from Grant No. R-151-000-032-112.

[1] C. Grebogi, E. Ott, and J. A. Yorke, Phys. Rev. Lett. **48**, 1507 (1982); Physica D **7**, 181 (1983).
[2] C. Grebogi, E. Ott, and J. A. Yorke, Phys. Rev. Lett. **57**, 1284 (1986); Phys. Rev. A **36**, 5365 (1987).
[3] C. Grebogi, E. Ott, and J. A. Yorke, Phys. Rev. Lett. **50**, 935 (1983); Ergod. Theory Dyn. Syst. **5**, 341 (1985).
[4] S. X. Qu, B. Christiansen, and D. R. He, Acta Phys. Sin. **44**, 841 (1995) (in Chinese).
[5] S. X. Qu and B. Christiansen, Phys. Lett. A **201**, 413 (1995).
[6] X. L. Ding, S. G. Wu, Y. C. Yin, and D. R. He, Chin. Phys. Lett. **16**, 167 (1999).
[7] B. Hu, B. Li, J. Liu, and Y. Gu, Phys. Rev. Lett. **82**, 4224 (1999).
[8] H.-S. Chen, Jiao Wang, and Y. Gu, Chin. Phys. Lett. **17**, 85 (2000).
[9] J. Wang, X. L. Ding, B. Hu, B. H. Wang, J. S. Mao, and D. R. He, Phys. Rev. E **64**, 026202 (2001).
[10] J. Wang, X. L. Ding, B. H. Wang, and D. R. He, Chin. Phys. Lett. **18**, 13 (2001).
[11] X. M. Wang *et al.*, Eur. Phys. J. D **19**, 119 (2002).
[12] Y. M. Jiang, Y. Q. Lu, X. G. Chao, and D. R. He, Eur. Phys. J. D **29**, 285 (2004).

[13] C. Mira, Int. J. Bifurcation Chaos Appl. Sci. Eng. **6**, 893 (1996).
[14] G. Hsu, E. Ott, and C. Grebogi, Phys. Lett. A **127**, 199 (1988).
[15] T. Tél, in *Directions in Chaos*, edited by B.-L. Hao, D.-H. Feng, and J.-M. Yuan (World Scientific, Singapore, 1991), Vol. 3.
[16] Y.-C. Lai and R. L. Winslow, Phys. Rev. Lett. **74**, 5208 (1995).
[17] J. P. Crutchfield and K. Kaneko, Phys. Rev. Lett. **60**, 2715 (1988).
[18] K. Kaneko, Phys. Lett. A **149**, 105 (1990).
[19] E. Ott, C. Grebogi, and J. A. Yorke, Phys. Rev. Lett. **64**, 1196 (1990); D. Auerbach, C. Grebogi, E. Ott, and J. A. Yorke, *ibid.* **69**, 3479 (1992).
[20] Y.-C. Lai and C. Grebogi, Phys. Rev. E **49**, 1094 (1994).
[21] H. G. Schuster, *Deterministic Chaos: An Introduction*, 3rd augmented ed. (VCH, Weinheim, 1995), pp. 18–19.
[22] B. V. Chirikov, Phys. Rep. **52**, 263 (1979).
[23] R. Blumel and W. P. Reinhardt, *Chaos in Atomic Physics* (Cambridge University Press, Cambridge, England, 1997), pp. 119–130.
[24] C. Grebogi, S. W. McDonald, E. Ott, and J. A. Yorke, Phys. Lett. **110A**, 1 (1985).
[25] D. K. Umberger and J. D. Farmer, Phys. Rev. Lett. **55**, 661 (1985).
[26] J. D. Farmer, in *Dimensions and Entropies in Chaotic Systems*, edited by E. Mayer-Kress (Springer, Berlin, 1986), p. 54.
[27] K. Falconer, *Fractal Geometry*, translated by W. Q. Zeng and S. Y. Liu (Northeast University Publishing, Shenyang, 1991) (in Chinese).
[28] E. Ott, *Chaos in Dynamical Systems* (Cambridge University Press, Cambridge, England, 1993), pp. 282–283.
[29] D. R. He (unpublished).